

1 **Phylogenetic relationships of a new titanosaur (Dinosauria, Sauropoda) from the**
2 **Upper Cretaceous of Uruguay**

3

4 MATÍAS SOTO^{1*}, JOSÉ L. CARBALLIDO², MAX C. LANGER³, JULIAN C.G.

5 SILVA JUNIOR³, FELIPE MONTENEGRO^{1,4}, DANIEL PEREA¹

6 ¹Instituto de Ciencias Geológicas, Facultad de Ciencias, Iguá 4225, 11400 Montevideo,

7 Uruguay, msoto@fcien.edu.uy

8 ²Museo Paleontológico Egidio Feruglio, Avenida Fontana 140, 9100 Trelew, Chubut,

9 Argentina

10 ³Departamento de Biología, FFCLRP, Universidade de São Paulo, Av. Bandeirantes

11 3900, 14040-901, Ribeirão Preto, Brazil

12 ⁴Museo Nacional de Historia Natural, Miguelete 1825, 11600 Montevideo, Uruguay

13

14

15 **ABSTRACT**

16 The up to 200 m thick Upper Cretaceous deposits of Uruguay includes from base to top

17 the Guichón, Mercedes, and Asencio formations, plus the lateral correlate of the latter,

18 the Queguay Formation. In 2006, the most complete sauropod from the country was

19 excavated from the Guichón Formation near Araújo, Paysandú Department. Augmented

20 by new specimens reported here, the material includes sixty caudal vertebrae (all strongly

21 procoelous, except for the biconvex first one), a partial coracoid, long bone fragments

22 (proximal and distal portions of tibia, proximal portion of fibula), two astragali, and six

23 metatarsals, as well as associated eggshell fragments. The Uruguayan titanosaur shows a
24 unique combination of characters (biconvex first caudal centrum, pneumatic foramina in
25 the anteriormost caudal centra, dorsal tuberosities on the transverse processes of the
26 anterior caudal vertebrae, well developed fibular knob, pyramidal astragalus), as well as
27 a potential autapomorphy – middle caudal centra condyles with hexagonal contour –
28 allowing the proposition of new genus and species, *Udelartitan celeste*. Phylogenetic
29 analyses were for the first time performed to assess the relations of that taxon, which was
30 recovered either as a saltosaurine saltosaurid or a non-saltosaurid saltasauroid. Further,
31 one of the analyses show *Udelartitan celeste* nested within a clade including Late
32 Cretaceous titanosaurs with a biconvex first caudal vertebra, such as *Alamosaurus*
33 *sanjuanensis*, *Baurutitan britoi*, and *Pellegrinisaurus powelli*. This contribution
34 demonstrates that at least two titanosaur lineages were present in the Late Cretaceous of
35 Uruguay: Saltasauroida and Aeolosaurini, the latter recently recognized in the
36 stratigraphically younger Asencio Formation.

37 Keywords: Late Cretaceous, Uruguay, Titanosauria, Guichón Formation

38 ***Corresponding author**

39 **INTRODUCTION**

40 With over 80 species, mainly described in this century, titanosaurs represent the most
41 successful and diverse sauropodomorph group (Carballido et al., 2022). They were the
42 most abundant large-bodied herbivorous in the Late Cretaceous of Gondwana, in strong
43 contrast with the ornithischian-dominated coeval faunas of Laurasia. The clade
44 apparently arose in South America (Gorscak and O'Connor, 2016), where it shows its
45 greatest diversity, with records ranging from the Berriasian–Valanginian to the
46 Maastrichtian (e.g., Silva Junior et al., 2019; Gallina et al., 2022).

47 In Uruguay, titanosaur remains are known since the beginning of the XX century,
48 when four species were recognized based on fragmentary remains (Huene, 1929).
49 Although such referrals have been questioned (Powell, 2003; Mannion and Otero, 2012;
50 Soto et al., 2012, 2022), their titanosaur identity is out of doubt given the strong procoely
51 of the caudal centra. These findings were relevant because they allowed to confirm the
52 presence of Upper Cretaceous rocks in Uruguay (Huene, 1929), although in light of recent
53 South American findings, e.g., *Ninjatitan zapatai* (Gallina et al., 2021), *Tapuiasaurus*
54 *macedoi* (Zaher et al., 2011), an older age within the Cretaceous cannot be ruled-out in
55 absence of additional data.

56 Most sauropod findings in Uruguay come from the Mercedes and Asencio
57 formations. Their exact stratigraphic provenance is, however, not always easy to define,
58 given the different lithostratigraphic arrangements proposed for the Uruguayan
59 Cretaceous (Soto et al., 2022) and because the fossils are usually not found in situ. Most
60 historical findings seem to come from the Asencio Formation (sensu Bossi, 1966),
61 including a caudal centrum referred to *Aeolosaurus* sp. (Soto et al., 2022), but some
62 fossils found in situ have been recently reported for the Mercedes Formation. For the
63 underlying Guichón Formation, the first titanosaur remains were found in this century,

64 when dozens of vertebrae and bone fragments were unearthed from a large gully (Figs.
65 1-2; Soto et al., 2008). Soto et al. (2012) described these fossils in more detail and
66 considered them to be closely related to *Alamosaurus sanjuanensis* and *Baurutitan britoi*.
67 However, a phylogenetic analysis including the entire set of remains testing this
68 hypothesis was never published, which is the prime aim of this contribution.

69

70 **GEOLOGICAL AND PALEOFAUNAL SETTING**

71 Bossi (1966) recognized three Cretaceous units in the Norte Basin, Uruguay (from base
72 to top): Guichón, Mercedes, and Asencio formations (Fig. 1). A fourth unit, Queguay
73 Formation (Goso & Bossi, 1966), has been recently included as a lateral correlate of the
74 Asencio Formation, given its recent Campanian–Maastrichtian absolute dating
75 (Veroslavsky et al., 2019). The Guichón Formation crops out in northwestern Uruguay,
76 Paysandú Department (Fig. 2). It comprises reddish, fine-grained wackes of arkosic
77 composition (Fig. 3C). Subordinated lithologies include conglomerates (Fig. 3B) with
78 calcedonia, basalt, and brown pelite clasts. These deposits are silicified in places and
79 bioturbation is locally abundant, indicating paleosol development. The sandstones and
80 conglomerates have been interpreted as deposited by fluvial channels flowing towards
81 the SW (Goso & Perea, 2004). Finer lithologies were deposited in floodplains and aeolian
82 reworking of fluvial bars is seen locally (e.g., Paso Hervidero).

83 The locality bearing the fossils described here is close to Araújo, Paysandú
84 Department. It corresponds to a large gully produced by erosion, which has been recently
85 stabilized by the growing of trees (Fig. 3A). As the orange sandstones of the Guichón
86 Formation are eroded, bone, eggshell, and wood fragments are found scattered on the
87 sand. A silicified conglomerate forms the bottom of the gullies and towards their margins
88 there are column-like structures, where the sandstones incorporated carbonate due to

89 palaeoedafic processes. These columns were mostly eroded around the gully and only
90 mound-like relics (formed by accumulation of sandstone blocks) survived. The recovered
91 fossils comprise abundant titanosaur skeletal remains (Fig. 4), mostly caudal centra,
92 locally associated with eggshell fragments.

93 Previously, the Guichón Formation has yielded only few other fossils, including several
94 skeletons of the notosuchian *Uruguaysuchus aznarezi* (Rusconi, 1933; Soto et al., 2011),
95 a few isolated iguanodontian teeth, and an indeterminate theropod tooth mistakenly
96 referred to Ornithomimidae (Huene, 1934; Soto et al., 2012).

97 The age of the Guichón Formation has been a matter of debate. Facies similarities with
98 the Migues Formation, Aptian–Albian of the Santa Lucía Basin, led Goso & Perea (2003)
99 to propose a late Early Cretaceous age, which is not contradicted by the affinities of
100 *Uruguaysuchus aznarezi* to *Araripesuchus*, a taxon with a broad (Aptian–Maastrichtian)
101 chronological range within the Cretaceous. If that is the case, the hiatus with the overlying
102 Campanian–Maastrichtian Mercedes Formation (Goso & Perea, 2003; Veroslavsky et al.,
103 2019) would have been significant. However, the presence of a titanosaur with a biconvex
104 first caudal vertebrae and of *Sphaerovum*-like eggshells led Soto et al. (2008, 2012) to
105 propose a younger age, i.e.: Late Cretaceous, for Guichón Formation.

106

107 MATERIALS AND METHODS

108 All titanosaur specimens previously described in Soto et al. (2012), plus new unpublished
109 remains from the same locality, were measured and photographed. An effort was made to
110 identify additional characters of taxonomic relevance, apart from those originally
111 reported one decade ago. The elements were identified as mainly pertaining to a single
112 individual (FC-DPV 1900), plus at least two additional bones that indicate the presence

113 of a second, younger one. However, we followed more conservative approach and
114 considered only three near-articulated vertebrae as the holotype (FC-DPV 3595; Fig. 4).

115 In order to estimate the body length of the holotype specimen (the only found in
116 near articulation), we correlated two continuous variables using a linear regression on R
117 environment (Development Core Team 2013): (1) the estimated total body lengths of four
118 exceptionally well-preserved titanosaurs, *Rapetosaurus krausei* (Rogers and Forster,
119 2001), *Overosaurus paradasorum* (Coria et al., 2013), *Dreadnoughtus schrani* (Lacovara
120 et al., 2014), and *Alamosaurus sanjuanensis* (Tykoski and Fiorillo, 2017); (2) the
121 anteroposterior length of the first three caudal centra of the Uruguayan taxon.

122 In order to infer the phylogenetic relations of the new taxon, two data sets were
123 analyzed, with the new taxon added to the taxon/character matrices of Cerda et al. (2022)
124 and Navarro et al. (2022), based on the scores of FC-DPV 1900 and 3595. Also, following
125 Silva Junior *et al.* (2022), *Trigonosaurus pricei* was pruned from the two data-sets, with
126 *Baurutiran britoi* re-scored based on the new set of specimens defined by those authors.
127 Both matrices (which can be accessed at doi:10.17632/nz79w2kwsb.1) were then
128 analysed with the software TNT version 1.6 (Goloboff et al., 2008), firstly under equally
129 weighted parsimony (EWA), but also employing extended implied weighting (IWA).
130 Following Goloboff et al. (2018), the IWA analysis was conducted using a k-value
131 (concavity constant; see Goloboff, 1993) of 9 and applied to the data-sets of Cerda et al.
132 (2022) and Navarro et al. (2022). All analyses were performed using New Technologies
133 tree search up to find 30 MPTS and with a tree memory space of 100.000. To produce the
134 “reduced consensus” trees, unstable taxa were identified using the “Pruned Tree” option
135 in TNT.

136 This published work and the nomenclatural acts it contains have been registered
137 in ZooBank, the online registration system for the International Code of Zoological

138 Nomenclature. The ZooBank LSIDs (Life Science Identifiers) is [https://](https://zoobank.org/NomenclaturalActs/CB981DBD-84DB-4DD5-AE20-29D96092D1C)
139 zoobank.org/NomenclaturalActs/CB981DBD-84DB-4DD5-AE20-29D96092D1C.

140 *Institutional abbreviations.* FC-DPV, Vertebrate Fossil Collection, Facultad de
141 Ciencias, Universidad de la República, Uruguay.

142

143 **SYSTEMATIC PALEONTOLOGY**

144 Sauropoda Marsh, 1878

145 Macronaria Wilson & Sereno, 1998

146 Titanosauriformes Salgado et al., 1997

147 Titanosauria Bonaparte and Coria, 1993

148 Lithostrotia Upchurch, Barrett & Dodson 2004

149 Saltasauroida França, Marsola, Riff, Hsiou & Langer, 2016 sensu Carballido et al. 2022

150

151 *Udelartitan celeste* gen. et sp. nov.

152

153 ***Etimology:*** The genus name derives from UdelaR, acronym of the Universidad de la
154 República, plus *titan*, after the Greek mythology giants, a common suffix of titanosaur
155 names. The specific epithet name *celeste* (Spanish for sky-blue) is the nickname of
156 Uruguayan teams in international sport competitions.

157 ***Diagnosis:*** *Udelartitan celeste* differs from all other known titanosaurs based on an
158 unique combination of features (autapomorphies marked with *), i.e.: biconvex first
159 caudal centrum, anterior caudal vertebrae with well-developed neural spines with a
160 quadrangular cross-section and well-developed postspinal lamina, pneumatic foramina in
161 the anteriormost caudal centra, anterior caudal vertebrae with dorsal tuberosities on the
162 transverse processes, middle caudal centra cotyles and /or condyles with an hexagonal

163 contour*, well developed fibular knob, pyramidal astragalus, and marked oblique ridges
164 in the anterior face of metatarsals I and II*.

165 **Holotype:** FC-DPV 3595 (Figs. 5-6). This set, identified as caudal vertebrae 1 to 3,
166 corresponds to the only near-articulated specimens.

167 **Referred material:** FC-DPV 1900 (lot; Figs. 7-12), sixty caudal vertebrae (all strongly
168 procoelous), a partial coracoid, long bone fragments (distal and proximal tibial portions,
169 proximal fibular portion), six metatarsals, and two astragali.

170 **Type locality and horizon:** Araújo, near Quebracho, Paysandú Department, Uruguay.
171 Guichón Formation, Upper Cretaceous of Uruguay (Veroslavsky et al., 2019).

172

173 DESCRIPTION

174 Some of the FC-DPV 1900 and 3595 elements were briefly described by Soto et al.
175 (2012), where complete measurements of all vertebrae are provided. Here we will
176 complement that study with newly recovered specimens and summarize characters of
177 phylogenetic significance from the complete set of remains.

178

179 Axial Skeleton

180 **Caudal vertebrae.** The tail elements are represented by the associated first three caudal
181 centra, plus anterior centra and neural arches, and middle to posterior caudal centra (with
182 some of the posteriormost recovered elements preserving the neural arch).

183 The first caudal centrum (Fig. 5) is deformed, so that the right lateral outline
184 appears anteroposteriorly shortened compared to the left one. This centrum is strongly
185 biconvex, with the anterior articular surface larger than the posterior (Fig. 5A). Biconvex
186 first caudal centra have been reported for several titanosaurs (e.g., *Alamosaurus*
187 *sanjuanensis*, *Baurutitan britoi*, *Dreadnoughtus schrani*, *Pellegrinisaurus powelli*;

188 Gilmore, 1946; Salgado, 1996; Salgado et al., 2005; Lacovara et al., 2014) most of which
189 currently considered saltasauroids. This includes *Neuquensaurus australis*, the last sacral
190 element of which could be considered homologous to the first caudal vertebra of
191 titanosaurs with fewer (six) sacral elements. In the Uruguayan material, the neural arch
192 of the first caudal vertebra is mostly lost, but the preserved proximal portion of the
193 transverse processes show that they were laterodorsally and slightly posteriorly directed.
194 The lateral, ventral, and dorsal surfaces of the centrum have several small foramen-like
195 hollows (Fig. 5A) that are related to the internal pneumaticity, as observed in Saltosaurini
196 (e.g., *Neuquensaurus australis*, *Rocasaurus muniozi*, *Saltasaurus loricatus*; Cerda et al.,
197 2012; Zurriaguz and Cerda, 2017).

198 Anterior, middle, and posterior caudal centra are strongly procoelous, as in most
199 Titanosauria, with few exceptions such as *Andesaurus delgadoi* or *Opisthocoelicaudia*
200 *skarzynskii* (e.g. Salgado et al., 1997). The condylar convexity indexes (Mannion et al.,
201 2019) range from 0.5 to 0.99 (see Table 1). Posteriormost caudal centra were not
202 recovered. Anterior caudal vertebrae are represented by several isolated centra that lack
203 the neural arches and two isolated neural spines. As in the first caudal element, some of
204 the anteriormost caudal centra present small foramina on their lateral surfaces. These are
205 subcircular, with diameters of around 0.5 cm. Similar foramina are present in some
206 Saltosauridae titanosaurs, such as *Alamosaurus sanjuanensis*, *Rocasaurus muniozi*, and
207 *Saltasaurus loricatus*. Additionally, as in these taxa, some of the anteriormost caudal
208 vertebrae (including the first one) present one or more foramina on their ventral surfaces.
209 One of the centra bears two anteroposteriorly elongated foramina, positioned close to the
210 midline of the element and on the anterior half of the ventral surface (Fig. 6B), with
211 smaller foramina at the posterior region of the ventral surface; which shape and position
212 are more reminiscent to the pneumatic foramina of some saltasauroids (e.g., *Alamosaurus*

213 *sanjuanensis*, *Saltasaurus loricatus*, *Pellegrinisaurus powelli*) than to the vascular
214 foramina present in several non-saltasauroid sauropods.

215 Few other anterior caudal elements present solely small foramina on their ventral surface.
216 As in other titanosaurs, we interpret the foramina present in *Uderlatitan celeste* as
217 pneumatic openings excavated by air sac diverticuli of the tail (Cerda et al., 2022; Taylor
218 and Wedel, 2021). Yet, except for the first element, it was not possible to recognize the
219 presence of internal pneumaticity in the caudal vertebrae (see above). Therefore, we
220 interpreted that the caudal pneumaticity do not reach the middle section of the tail,
221 contrasting with the condition in some Saltosaurini, which bear pneumatic foramina up
222 to the posterior caudal elements. In fact, internal pneumatic cavities are widespread within
223 that clade, even when no external openings are present (Zurriaguz and Cerda, 2017). The
224 ventral surfaces of the FC-DPV 1900 tail vertebrae are anteroposteriorly and transversally
225 concave and mediolaterally narrow. The preserved transverse processes of the anterior
226 caudal vertebrae are triangular, wider at their base and narrower towards the distal end,
227 as common among non-diplodocoid sauropods, with the exception of some Lognkosauria
228 (e.g., *Patagotitan mayorum*, *Futalognkosaurus dukei*). The few preserved transverse
229 processes are posteriorly inclined as in titanosauriforms and related forms. A marked
230 dorsal tuberosity in the transverse process is present in two of the best preserved anterior
231 caudal vertebrae (Figs. 6E, F), a rather widespread character.

232 A horizontal ridge in the middle caudal centra (Fig. 7A, F) is interpreted as
233 homologous to this dorsal tuberosity. Middle caudal centra show cotyles and/or condyles
234 with a hexagonal contour (Fig. 7D-E, I-J). The posterior caudal centra are
235 anteroposteriorly elongated, with convex lateral and ventral surfaces. Their cotyles are
236 less excavated and condyles more gracile than those of the previous vertebrae. One of the
237 posterior caudal centra also shows a cotyle with hexagonal contour (Fig. 8F).

238 Two isolated neural spines briefly described, but not figured by Soto et al. (2012)
239 are herein identified as anterior caudal neural spines (Fig. 9), based upon comparisons
240 with more complete titanosaur tails (e.g., *Baurutitan britoi*). Their bases are quadrangular
241 in cross-section, with similar anteroposterior and lateromedial breadths. Distally, the
242 neural spine is somewhat broader lateromedially, although the postspinal lamina is
243 broken. Hence, it can be better described as quadrangular rather than lateromedially
244 expanded, like that of most non-colossosaur titanosaurs (Carballido et al., 2017). The
245 postzygapophyseal facets are roughly elliptic in shape, similar to those of the anterior
246 caudal elements of *Caieiria allocaudata* (Silva Junior et al., 2022:fig. 21), but lacking a
247 hyposphenal ridge. The prezygapophyses are not preserved and the
248 spinoprezygapophyseal lamina seems to be reduced; i.e., medially bound by the prespinal
249 lamina, resembling the lamination pattern of *Caieiria allocaudata*. The lateral edge of the
250 neural spine is formed by the robust and well-marked spinopostzygapophyseal lamina
251 (Fig. 9) and its anterior and posterior surfaces bear pre- and postspinal laminae. The later,
252 flanked by the spinopostzygapophyseal laminae, is broken, but was clearly robust. The
253 prespinal lamina is equally robust and not distally expanded, unlike the condition in
254 lognkosaurs (Carballido et al., 2017). Although the neural spine is distally broken, the
255 lateral edges, formed by the spinopostzygapophyseal lamina, show the beginning of a
256 lateromedial expansion.

257

258 Appendicular Skeleton

259 *Pectoral girdle*. A partially preserved left coracoid was mentioned, but not figured by
260 Soto et al. (2012). For descriptive purposes the coracoid is described as if the scapula-
261 coracoid was horizontally oriented. Although incomplete, the bone is subquadrangular
262 in lateral/medial views (Fig. 11A). The scapular articulation is not preserved, but the

263 bone seems to be relatively short anteroposteriorly, unlike the longer coracoid of several
264 titanosaurs, which an anteroposterior length around twice the breadth of the scapular
265 articular surface. The anteroventral margin of the bone is rectangular, as common in
266 saltosaurids and few other titanosaurs (e.g., *Quetecsaurus rusconii*, *Patagotitan*
267 *mayorum*; González Riga et al., 2019; Otero et al., 2020). The glenoid is well preserved
268 and a marked groove is seen right anterior to it, also seen in most camarasauromorphs
269 (e.g., *Tehuelchesaurus benitezii*, *Xianshanosaurus shijiagouensis*, *Patagotitan*
270 *mayorum*, *Neuquensaurus australis*). Yet, the infraglenoid groove ends without forming
271 a marked infraglenoid lip, as also observed in some titanosaurs, including non-
272 Saltosauridae Saltasauroida (e.g., *Isisaurus colberti*). The coracoid foramen (Fig. 11A)
273 is positioned at the posterodorsal margin of the bone.

274 *Hindlimb*. Proximal and distal left tibial ends are preserved; the former damaged and not
275 mentioned by Soto et al. (2012). The proximal end of the tibia is transversally expanded,
276 as in most sauropods, and bears a cnemial crest that is, at its base, anterolaterally oriented
277 (Fig 11B). The crest is proximally broken, better preserved more distally, forming a
278 marked concavity where the fibula articulates. The distal end of the tibia is markedly
279 expanded (Fig. 11) compared to the partial mid-shaft, an apomorphic condition among
280 titanosaurs. The medial malleolus (*sensu* Poropat et al. 2015) is short and robust, whereas
281 the lateral malleolus (*sensu* Poropat et al. 2015), which articulates to the ascending
282 process of the astragalus, is around twice longer, but more gracile. This resembles the
283 morphology of saltosaurinae titanosaurs (e.g., *Saltasaurus loricatus*, *Neuquensaurus*
284 *australis*; Otero, 2010), contrasting with the equally developed malleoli of most other
285 sauropods, including several titanosaurs (e.g., *Bonitasaura salgadoi*, *Dreadnoughtus*
286 *schrani*).

287 Only the proximal portion of a right fibula is preserved. The element is robust and
288 mediolaterally expanded. The proximal articulation is slightly convex and with a rugose
289 surface. It shows a gracile anteromedial ridge, that projects anterolaterally. This ridge was
290 defined as the anterior crest of the fibula, which extends medially and becomes
291 sandwiched between the cnemial crest and the body of the tibia (Wilson and Upchurch,
292 2009) which is a widespread character amongst titanosauriforms, with some exceptions
293 among saltosaurids (*Saltasaurus loricatus*, *Neuquensaurus australis*; D’Emic, 2012). A
294 marked fibular knob, extending anterodistally from the posteroproximal border, is present
295 on the medial surface of the fibula. The knob has a squared anterior outline and expands
296 distally as a thin lamina. The presence of this knob resulted in a posteriorly expanded
297 proximal margin of the fibula, so that its presence can be recognized in medial and
298 proximal views (Fig. 11). A similarly developed fibular knob was described for
299 *Uberabatitan ribeiroi* (Silva Junior et al. 2019) and seems to be also present in
300 *Bonitasaura salgadoi* (Gallina and Apesteguía, 2015), *Rapetosaurus krausei* (Curry
301 Rogers, 2009), *Sauroposeidon proteles* (Rose, 2007). It borders both a lateral and medial
302 fossae, with the latter deeper than the former.

303 Two right astragali were recovered (Fig. 12). Both have a triangular distal
304 outline, with bevelled posterolateral and posteromedial margins. Both tibial and fibular
305 articulations are marked by well-developed concavities, with the latter larger than the
306 former. The distal surfaces of the astragali are rugose and anteriorly curved. Both
307 astragali are almost as wide as long (Table 1), with the ascending process positioned at
308 the anterior margin, two characters widespread among latter eusauropods. As in most
309 macronarians, the distolateral lip of the astragalus is absent (Mannion et al., 2013). A
310 relatively small dorsal fossa is present on the posteromedial surface of the astragalus
311 (Fig. 12C). As in non-diplodocoid sauropods, the fibular facet of the astragalus faces

312 laterally, instead of posterolaterally (Whitlock, 2011). The posterior fossa is undivided,
313 resembling the condition of other titanosaurs (e.g., *Opisthocoelicaudia skarzynskii*,
314 *Neuquensaurus australis*, *Diamantinasaurus matildae*, *Pellegrinisaurus powelli*)

315 The metatarsals were identified, based on comparisons with complete pedes, such
316 as those of the “La Invernada” titanosaur (González Riga et al., 2008) and *Rapetosaurus*
317 *krausei* (Curry-Rogers, 2009), as left I, III, IV, and V, and right I and II. Their proximal
318 ends are lateromedially expanded with the articular surfaces slightly concave. Those are
319 angled ventromedially on both metatarsals I and perpendicular to the shaft on the
320 remaining ones. Proximally, small concavities mark the articulation facets with the
321 neighbouring metatarsals. Metatarsals I and II show a conspicuous oblique ridge
322 projecting medially. The distal ends are dorsoventrally expanded and have rounded and
323 rugose articular surfaces which are slightly angled dorsomedially on all elements..
324 Metatarsal I is somewhat damaged, but is clearly a robust element (Table 1). Its proximal
325 and distal articulations are wide, with the distal one almost as lateromedially wide as
326 anteroposteriorly long. Metatarsals II are also robust (see Table 1), but with proximal and
327 distal articulations more compressed than those of metatarsal I.

328 Elements interpreted as osteoderms by Soto et al. (2012) are flat, discoidal
329 structures of the same size and shape. Yet, a thin section of one of the best-preserved of
330 those elements rejected their organic nature (I. Cerda, pers. comm, 2022)., revealing that
331 they are most probably concretions

332

333 **DISCUSSION**

334 The regressions detailed in the “Material and Methods” indicate that *Udelartitan celeste*
335 was a small-sized titanosaur, measuring from 15 to 16 meters. Its titanosaur affinity is
336 suggested by several anatomical traits, such as strongly procoelous vertebrae spanning

337 throughout the tail, a condition known only in (most) titanosaurs and (several)
338 mamenchisaurids. Also, the placement of the neural arches in the anterior half of the
339 centra, the transverse expansion of the distal end of the tibia, and the pyramidal astragalus
340 are common features of titanosaurs (Salgado et al., 1997; Wilson, 2002). More
341 specifically, a biconvex first caudal centrum is only present in few taxa, including
342 *Alamosaurus sanjuanensis*, *Baurutitan britoi*, *Dreadnoughtus schrani*, and
343 *Pellegrinisaurus powelli* (Gilmore, 1946; Salgado, 1996; Campos et al., 2005; Lacovara
344 et al., 2014), whereas in *Neuquensaurus australis* this was incorporated as the seventh
345 sacral vertebra (Salgado et al., 2005). The conspicuous ridge in metatarsal I is similar to
346 that of *Neuquensaurus australis* (Otero, 2010). Finally, the caudal centra lack the
347 eccentric condyles and the anteriorly tilted anterior faces that characterize vertebrae
348 similar to those of *Aeolosaurus* spp, like that described by Soto et al. (2022) for the
349 Asencio Formation. The apparent anterior tilt in an anterior caudal vertebra of *Udelartitan*
350 *celeste* (Fig. 6) is likely due to breakage of its anteroventral portion.

351 Both Saltosaurinae and Saltasauroida appear to be a Gondwanan radiation of
352 titanosaurian sauropods, with the single exception of the North American *Alamosaurus*
353 *sanjuanensis*. The new taxon described here reinforces the idea that a great diversification
354 of saltasauroids (or even saltosaurines, depending on the analysis) took place in
355 Gondwana, especially in South America. This supports the hypothesis that saltasauroids
356 dispersed from South to North America at the end of the Cretaceous (dispersion events
357 also were responsible for the arrival of hadrosaurid ornithopods in South America; Estes
358 & Baéz, 1985). It is interesting to highlight the small size of the saltasauroids (including
359 *Udelartitan celeste*) nested together with the larger *Alamosaurus sanjuanensis*, in the
360 phylogenetic analyses conducted here. It is tempting to suggest that such larger size could
361 have resulted from titanosaurs arriving to an ecosystem with vacant niches or with an

362 improved capacity of exploring niches previously occupied by the dominant herbivores
363 from the Northern hemisphere (i.e., ornithischians).

364 The discovery of a saltauroid/saltosaurine in Uruguay with a biconvex first caudal
365 vertebra allows establishing correlations with other stratigraphic units in southern South
366 America: the Argentinean Neuquén Group and the Brazilian Baurú Group (Fig. 15).
367 Taking into account that araripesuchids and early-branching iguanodontians are also
368 found in the Guichón Formation, the lack of data regarding theropods and turtles hampers
369 correlation with the Cretaceous tetrapod assemblages of the Neuquén Group (Fig. 15;
370 Leanza et al., 2004). On one hand, the presence of araripesuchids and iguanodontians
371 recall the Limayan assemblage (Cenomanian-Early Turonian), although no remains of
372 rebbachisaurids, carcharodontosaurids or abelisaurids have so far been found in the
373 Guichón Formation. On the other hand, the presence of a saltasauroid/saltosaurine recall
374 the Coloradoan assemblage (Santonian-Early Campanian). In turn, the younger Asencio
375 Formation correlates with the Allenian assemblage (Late Campanian-Early
376 Maastrichtian) due to the presence of *Aeolosaurus*. As for the Baurú Group, forms related
377 to *Udelartitan celeste* include *Ibirania parva* and *Baurutitan britoi*. The former was found
378 in the São José do Rio Preto Formation (Santonian-Campanian), along with abelisaurid
379 and putative megaraptoran theropods, and notosuchian crocodyliforms. *Baurutitan britoi*,
380 in turn, comes from the Serra da Galga Formation (Maastrichtian) where it coexisted with
381 other titanosaurs (e.g., *Uberabatitan ribeiroi*, *Caieria allocaudata*), abelisaurid and
382 dromaeosaurid theropods, and peirosaurid and notosuchian crocodyliforms. The scarcity
383 of fossils from the Guichón Formation precluded more detailed comparisons.

384

385 **Phylogenetic analysis**

386 The description of *Udelartitan celeste* led to the identification of two new characters
387 based on the epipodial anatomy. The first relates to the anteroposterior length of distal
388 malleoli of the tibia, which can be about the same size (0) or the lateral malleolus can be
389 longer than the medial (1). The second character corresponds to the absence (0) or
390 presence (1) of a fibular knob in the posteromedial edge of the proximal end of the fibula.
391 These were added to both data-sets used here, as characters 432 and 433 for Cerda et al.
392 (2021) and 436 and 437 for Navarro et al. (2022).

393 The EWA analysis of the dataset modified from Cerda et al. (2021) retrieved
394 100,000 MPTs (collapsing tree memory) of 1,570 steps. The strict consensus of those
395 trees (see Supplementary Material) shows a large polytomic clade, forming a trichotomy
396 with *Epachthosaurus sciuttoi* and *Choconsaurus baileywillisi*. That polytomy mainly
397 results from the unstable position of several titanosaurs, as identified by the “Pruned
398 Tree” option in TNT, i.e., *Bonitasaura salgadoi*, *Caieiria allocaudata*, *Isisaurus colberti*,
399 *Nemegtosaurus mongoliensis*, *Ninjatitan zapatai*, *Notocolossus gonzalezparejasi*,
400 *Nullotitan glaciaris*, *Opisthocoelicaudia skarzynskii*, *Puertasaurus reuili*, and
401 *Tapuiasaurus macedoi*. Once these taxa are pruned from the MPTs, the reduced strict
402 consensus tree (Fig. 14a) is better resolved, although some taxa, i.e., *Diamantinasaurus*
403 *matildae*, *Dreadnoughtus schrani*, and *Malawisaurus dixeyi*, are still recovered in a
404 polytomy with the Saltasauroida and Colossosauria branches. In fact, that polytomy
405 precludes applying the phylogenetic definitions of those clades by Carballido et al.
406 (2022). *Udelartitan celeste* is placed in another polytomy in the saltasauroid branch,
407 together with *Alamosaurus sanjuanensis*, *Pellegrinisaurus powelli*, *Rapetosaurus*
408 *krausei*, and two minimal clades composed of *Uberabatitan ribeiroi* plus *Baurutitan*
409 *britoi*, and *Neuquensaurus australis* plus *Saltasaurus loricatus*.

410 In the second analysis (IWA) we recovered 100,000 MPTs (collapsing tree
411 memory) of 36.01846 steps. The strict consensus of these trees (see Supplementary
412 Material) recovered an early branching lineage of non-eutitanosaur titanosaurs (e.g.,
413 *Diamantinasaurus matildae*, *Isisaurus colberti*, *Malawisaurus dixeyi*, *Ninjatitan zapatai*,
414 *Notocolossus gonzalezparejasi*, and *Nullotitan glaciaris*), most of which were recovered
415 in the Saltasauroida branch in previous analyses of this dataset and also as unstable taxa
416 in the EWA analysis conducted here (see above). A large polytomy is sister to that
417 lineage, including thirteen species plus the Rinconsauria and Lognkosauria+*Bonitasaura*
418 *salgadoi* lineages. The reduced strict consensus tree (after pruning *Nemegtosaurus*
419 *mongoliensis* and *Caieiria allocaudata*) is well resolved (Fig. 14b), recovering
420 Saltasauroida and Colossosauria *sensu* Carballido et al. (2022), the latter formed by
421 Rinconsauria and Lognkosauria+*Bonitasaura salgadoi*. Irrespective of the topological
422 differences between the EWA and IWA trees, *Uderlatitan celeste* is positioned as a
423 saltasauroid and, in the latter, within a clade including titanosaurs mostly bearing a
424 biconvex first caudal centrum.

425 The analysis of the Navarro et al. (2022) data-set, with the inclusion of *Udelartitan*
426 *celeste*, resulted in 100,000 MPTs (collapsing tree memory) of 1,858 steps under EWA
427 and 5 MPTs of 4,217,529 steps under IWA. The strict consensus tree under EWA shows
428 a huge polytomy of titanosaurs (see Supplementary Material), which can be improved if
429 eight OTUs (*Argentinosaurus huinculensis*, *Bonitasaura salgadoi*, *Epachthosaurus*
430 *sciuttoi*, *Kaijutitan maui*, *Paludititan natalzensis*, *Patagotitan mayorum*, *Tapuiasaurus*
431 *macedoi*, and BIBE 45854), are pruned from the MPTs. In that three (Fig. 14c),
432 *Malawisaurus dixeyi* is the sister-taxon to a clade composed of two major titanosaur
433 branches, with *Udelartitan celeste* deeply nested within that including *Saltasaurus*
434 *loricatus*; although the pruning of *Patagotitan mayorum* prevents employing

435 Saltasauroida *sensu* Carballido et al. (2022). Note that in that topology, Saltosaurinae
436 includes *Alamosaurus sanjuanensis*, *Bonatitan reigi*, *Ibirania parva*, *Neuquensaurus*
437 *australis*, *Rocasaurus muniozi*, *Saltasaurus loricatus*, and BIBE 45854, many of which
438 are not traditionally nested within that group. The strict consensus of the 5 MPTs of the
439 EWA analysis (Fig. 14d) shows an uncommon arrangement, with *Patagotitan mayorum*
440 outside a clade including most eutitanosaurs. Hence, Saltasauroida *sensu* Carballido et
441 al. (2022) forms the bulk of titanosaurs, with Saltosaurinae including *Udelartitan celeste*
442 in an arrangement similar to that of the IWA reduced consensus.

443 The position here recovered for *Udelartitan celeste* results from the recognition
444 of several apomorphic characters present in the new titanosaur; the numbers of which
445 follow the matrix of Cerda et al. (2022). It shares with most titanosaurs a posteriorly
446 convex articular surface of the first caudal vertebra (ch. 225); with reversions such as in
447 *Opisthocoelicaudia skarzynskii*, the articular surface of which is concave. Also, as in most
448 titanosaurs, except for early diverging taxa such as *Andesaurus delgadoi* or *Malawisaurus*
449 *dixeyi*, the anterior caudal vertebrae of *Udelartitan celeste* are strongly procoelous (ch.
450 231). Two apomorphic characters of Eutitanosauria (Fig. 14b) are also present in
451 *Udelartitan celeste*, i.e.: strongly procoelous posterior caudal vertebrae (ch. 261) and a
452 marked knob at the posteromedial edge of the proximal end of the fibula (ch. 437). As in
453 other saltasauroids, the ventral surface of the anterior caudal centra of *Udelartitan celeste*
454 are transversely concave (ch. 233). In the analyses were *Udelartitan celeste* is nested
455 within Saltosauridae, this position is supported by an astragalus as long as wide (chs. 372,
456 378) and a biconvex first caudal vertebra (ch. 224, 225). Equally, its nesting within
457 Saltosaurinae is supported by middle caudal vertebrae more than twice longer than the
458 height of the centrum (ch. 259), as also seen in *Alamosaurus sanjuanensis*, *Saltasaurus*
459 *loricatus*, and *Neuquensaurus australis*, and a distal lateral malleolus of the tibia longer

460 than the medial malleolus (ch. 436). Conversely, *Udelartitan celeste* differs from some
461 saltosaurines such as *Alamosaurus sanjuanensis*, *Saltasaurus loricatus*, and *Rocasaurus*
462 *muniozi*, because its posterior caudal centra are subcircular in cross section (ch. 262), and
463 not strongly dorsoventrally compressed as in those taxa.

464

465 **CONCLUSIONS**

466 *Udelartitan celeste* gen. et sp. nov. represents a second sauropod taxon recognized in
467 Uruguay, after the recently reported *Aeolosaurus* vertebra from the Asencio Formation
468 (Soto et al., 2022). Its phylogenetic relations as either a saltosaurine saltosaurid or a non-
469 saltosaurid saltasauroid documents the presence of saltasauroids in the Guichón
470 Formation. The close relation with taxa such as *Pellegrinisaurus powelli*, *Baurutitan*
471 *britoi*, and *Alamosaurus sanjuanensis* hypothesized by Soto et al (2012) was partially
472 recovered in some of the trees. Irrespective of the topologies, *Udelartitan celeste* is
473 retrieved within clades formed solely by late Late Cretaceous taxa. This does not
474 necessarily imply this age for the Guichón Formation, but hints into such an inference.

475

476 **Acknowledgements**

477 Alejandra Rojas (Facultad de Ciencias, UDELAR) is acknowledged for access to
478 specimens under her care. Rodolfo Beasley and Iván Grela (UPM) allowed collecting of
479 specimens and provided valuable logistic support. Juan Ignacio Cerda kindly examined a
480 putative osteoderm. Phillip Mannion and two anonymous reviewers contributed to
481 improve an original draft of this paper. Funding: CSIC/UdelaR Grupo I+D Paleontología
482 de Vertebrados (C302/347, responsables: Daniel Perea and Martín Ubilla) and FAPESP
483 20/07997-4 (responsable: Max Langer).

484

485 **Literature cited**

- 486 Bonaparte, J.L. & Coria, R. 1993. Un nuevo y gigantesco sauropodo titanosaurio de la
487 Formacion Rio Limay (Albiano-Cenomaniano) de la Provincia del Neuquen,
488 Argentina. *Ameghiniana* 30(3):271–282.
- 489 Bossi, J. 1966. *Geología del Uruguay*. Departamento de Publicaciones de la Universidad
490 de la República, Montevideo. 469 pp.
- 491 Campos, D.A.; Kellner, A.W.A.; Bertini, R.J.; Santucci, R.M. 2005. On a titanosaurid
492 (Dinosauria, Sauropoda) vertebral column from the Bauru Group, Late Cretaceous
493 of Brazil. *Arquivos do Museu Nacional*. **63** (3):565–593.
- 494 Carballido J.L., Pol, D., Otero A., Cerda I., Salgado L., Garrido A., Ramezzani J., Cúneo
495 N. Krause M. 2017. A new giant titanosaur sheds light on body mass evolution
496 amongst sauropod dinosaurs. *Proceedings of the Royal Society, B*. 284:
497 20171219.20171219.
- 498 Carballido, José L.; Otero, Alejandro; Mannion, Philip D.; Salgado, Leonardo & Pérez
499 Moreno, Agustín 2022. Titanosauria: A Critical Reappraisal of Its Systematics and
500 the Relevance of the South American Record". In Otero, Alejandro; Carballido, José
501 L.; Pol, Diego (eds.). *South American Sauropodomorph Dinosaurs*. Springer
502 International Publishing. pp. 269–298.
- 503 Cerda, I., Zurriaguz, V.L., Carballido, J.L., González, R., & Salgado, L. 2021. Osteology,
504 paleohistology and phylogenetic relationships of *Pellegrinisaurus*
505 *powelli* (Dinosauria: Sauropoda) from the Upper Cretaceous of Argentinean
506 Patagonia. *Cretaceous Research*. 128: 104957. doi:10.1016/j.cretres.2021.104957
- 507 Curry Rogers, K. 2009. The postcranial osteology of *Rapetosaurus krausei* (Sauropoda:
508 Titanosauria) from the Late Cretaceous of Madagascar. *Journal of Vertebrate*
509 *Paleontology* 29(4):1046-1086.

- 510 Curry Rogers, K.; Forster, C.A. 2001. The last of the dinosaur titans: a new sauropod
511 from Madagascar. *Nature*. 412(6846):530–534.
- 512 D’Emic, M.D. 2012. The early evolution of titanosauriform sauropod dinosaurs.
513 *Zoological Journal of the Linnean Society* 166:624–671.
- 514 Estes, R., & Báez, A. 1985. Herpetofaunas of North and South America during the Late
515 Cretaceous and Cenozoic: Evidence for Interchange? The Great American Biotic
516 Interchange, 139–197.
- 517 França, M.A.G.; Marsola, J.C.d A.; Riff, D.; Hsiou, A.S. & Langer, M.C. 2016. New
518 lower jaw and teeth referred to *Maxakalisaurus topai* (Titanosauria: Aeolosaurini)
519 and their implications for the phylogeny of titanosaurid sauropods. *PeerJ*. 4: e2054.
- 520 Gallina, P.A. & Apesteguía, S. 2015. Postcranial anatomy of *Bonitasaura*
521 *salgadoi* (Sauropoda, Titanosauria) from the Late Cretaceous of Patagonia. *Journal*
522 *of Vertebrate Paleontology* e924957
- 523 Goloboff, P. 1993. Estimating carácter weights during tree search. *Cladistics* 9:83-91.
- 524 Goloboff, P.; Farris, J.S. & Nixon, K.C. 2008. TNT, a program for phylogenetic analysis.
525 *Cladistics* 24:774-786.
- 526 Gorscak, E. & O’Connor, P.M. 2016. Time calibrated models support congruency
527 between Cretaceous continental rifting and titanosaurian evolutionary history.
528 *Biological Letters* 122015104720151047
- 529 Gallina, P. A.; Canale, J.I. & Carballido, J.L. 2021. The Earliest Known Titanosaur
530 Sauropod Dinosaur". *Ameghiniana*. **58** (1): 35–51. Gilmore, C.W. 1946. Reptilian
531 fauna of the North Horn Formation of central Utah. *U.S. Geological Survey*
532 *Professional Paper*. 210-C:29-51.

- 533 González Riga, B.J., Calvo, J.O. y Porfiri, J. 2008. An articulated titanosaur from
534 Patagonia (Argentina): new evidences of the pedal evolution. *Palaeoworld* 17: 33-
535 40.
- 536 González Riga, B. J.; Lamanna, M. C.; Otero, A.; Ortiz David, L. D.; Kellner, A. W. A.;
537 Ibiricu, L. M. 2019. An overview of the appendicular skeletal anatomy of South
538 American titanosaurian sauropods, with definition of a newly recognized
539 clade. *Anais da Academia Brasileira de Ciências* 91(suppl 2):
540 e20180374. doi:10.1590/0001-3765201920180374
- 541 Goso, H. & Bossi, J. Cenozoico. In: Bossi, J. (ed.) Geología del Uruguay, Departamento
542 de Publicaciones de la Universidad de la República, Montevideo, p. 259-301, 1966.
- 543 Goso, C.A. & Perea, D. El Cretácico post-basáltico de la Cuenca Litoral del Río Uruguay:
544 geología y paleontología. In: Veroslavsky, G.; Ubilla, M.; Martínez, S. (eds.),
545 Cuencas sedimentarias de Uruguay: geología, paleontología y recursos minerales –
546 Mesozoico. DIRAC, Facultad de Ciencias, Montevideo, p. 141-169, 2003.
- 547 Huene, F. von. 1929. Terrestrische Oberkreide in Uruguay. *Zentralblatt für Geologie,*
548 *Mineralogie und Paläontologie*, v. Ab. B 4:107-112.
- 549 Huene, F. von. 1934. Nuevos dientes de Saurios del Cretácico del Uruguay. *Boletín del*
550 *Instituto Geológico del Uruguay*, 21:13-20.
- 551 Lacovara, K.J.; Ibiricu, L.M.; Lamanna, M.C.; Poole, J.C.; Schroeter, E.R.; Ullmann,
552 P.V.; Voegele, K.K.; Boles, Z.M.; Egerton, V.M.; Harris, J.D.; Martínez, R.D.;
553 Novas, F.E. 2014. A Gigantic, Exceptionally Complete Titanosaurian Sauropod
554 Dinosaur from Southern Patagonia, Argentina. *Scientific*
555 *Reports*. doi:10.1038/srep06196.

- 556 Leanza H.A., Apesteguía S., Novas F.E. & De la Fuente M.S., 2004. Cretaceous terrestrial
557 beds from the Neuquén basin (Argentina) and their tetrapod assemblages. –
558 Cretaceous Research 25: 1-96.
- 559 Mannion P.D. & Otero, A. 2012. A reappraisal of the Late Cretaceous Argentinean
560 sauropod dinosaur *Argyrosaurus superbus*, with a description of a new titanosaur
561 genus, Journal of Vertebrate Paleontology 32: 614-638.
- 562 Marsh, O.C. 1878. Principal characters of American Jurassic dinosaurs. Part I. *American*
563 *Journal of Science and Arts* 16(95): 411–416.
- 564 Navarro, B. A.; Ghilardi, A. M.; Aureliano, T.; Díaz, V. D.; Bandeira, K. L. N.;
565 Cattaruzzi, A. G. S.; Iori, F. V.; Martine, A. M.; Carvalho, A. B.; Anelli, L. E.;
566 Fernandes, M. A.; Zaher, H. 2022. A new nanoid titanosaur (Dinosauria: Sauropoda)
567 from the Upper Cretaceous of Brazil. *Ameghiniana* 59(5):317–354.
- 568 Otero, A. 2010. The appendicular skeleton of *Neuquensaurus*, a Late Cretaceous
569 saltasaurine sauropod from Patagonia, Argentina». *Acta Palaeontologica*
570 *Polonica* 55 (3): 399-426. doi:10.4202/app.2009.0099
- 571 Poropat, S.F.; Upchurch, P.; Mannion, P.D.; Hocknull, S.A.; Kear, B.P.; Sloan, T.;
572 Sinapius, G.H.K.; Elliot, D.A. 2014. Revision of the sauropod
573 dinosaur *Diamantinasaurus matildae* Hocknull et al. 2009 from the mid-Cretaceous
574 of Australia: Implications for Gondwanan titanosauriform dispersal. *Gondwana*
575 *Research*. 27(3): 995–1033. doi:10.1016/j.gr.2014.03.014.
- 576 Powell, J.E. 2003. Revision of South American Titanosaurids Dinosaurs:
577 Palaeobiological, Palaeobiogeographical and Phylogenetic Aspects. Records of the
578 Queen Victoria Museum, 111, 1-173.

- 579 Rose, Peter J. 2007. A new titanosauriform sauropod (Dinosauria: Saurischia) from the
580 Early Cretaceous of central Texas and its phylogenetic relationships. *Palaeontologia*
581 *Electronica*. 10(2), 65 pp.
- 582 Salgado, L. 1996. *Pellegrinisaurus powelli* nov. gen. et sp. (Sauropoda, Titanosauridae)
583 from the Upper Cretaceous of Lago Pellegrini, Northwestern Patagonia,
584 Argentina. *Ameghiniana*. **33** (4): 355–365.
- 585 Salgado, L.; Coria, R.A.; Calvo, J.O. 1997a. Evolution of Titanosaurid Sauropods. I:
586 Phylogenetic analysis based on the postcranial evidence. *Ameghiniana*, Vol. 34, p.
587 3-32.
- 588 Salgado, L.; Apesteguía, S. & Heredia, S.E. 2005. A New Specimen of *Neuquensaurus*
589 *australis*, a Late Cretaceous Saltasaurine Titanosaur from North Patagonia. *Journal*
590 *of Vertebrate Paleontology* 25(3): 623-634. Silva Junior et al., 2019
- 591 Silva Junior, J.C., Martinelli, A.G., Marinho, T.S., da Silva, J.I. & Langer, M.C.
592 2022. New specimens of *Baurutitan britoi* and a taxonomic reassessment of the
593 titanosaur dinosaur fauna (Sauropoda) from the Serra da Galga Formation (Late
594 Cretaceous) of Brazil. *PeerJ*. 10. e14333. doi:10.7717/peerj.14333
- 595 Soto, M.; Perea, D.; Veroslavsky, G.; Rinderknecht, A; Ubilla, M. & Lecuona, G. 2008.
596 Nuevos hallazgos de restos de dinosaurios y consideraciones sobre la edad de la
597 Formación Guichón. *Revista de la Sociedad Uruguaya de Geología* 15:11-23.
- 598 Soto, M.; Pol, D. & Perea, D. 2011. A new specimen of *Uruguaysuchus aznarezi*
599 (Crocodyliformes: Notosuchia) from the Cretaceous of Uruguay and its phylogenetic
600 relationships. *Zoological Journal of the Linnean Society, Special Issue 1st Symposium*
601 *on the Evolution of Crocodyliforms*, 163:S173-S198. doi:10.1111/j.1096-
602 3642.2011.00717.x

- 603 Soto, M.; Perea, D. & Cambiaso, A. 2012. First sauropod (Dinosauria: Saurischia)
604 remains from the Guichón Formation, Late Cretaceous of Uruguay. *Journal of South*
605 *American Earth Sciences*, 33(1):68-79. doi:10.1016/j.jsames.2011.08.003
- 606 Soto, M.; Montenegro, F.; Mesa, F. & Perea, D. 2022. Sauropod (Dinosauria: Saurischia)
607 remains from the Mercedes and Asencio formations (sensu Bossi, 1966), Upper
608 Cretaceous of Uruguay. *Cretaceous Research* 131:105072.
- 609 Taylor, M. P. & Wedel, M.J. 2021. Why is vertebral pneumaticity in sauropod dinosaurs
610 so variable? (version 3) *Qeios* 1G6J3Q.5. doi: 10.32388/1G6J3Q.
- 611 Tykoski, R.S. & Fiorillo, A. R. 2017. An articulated cervical series of *Alamosaurus*
612 *sanjuanensis* Gilmore, 1922 (Dinosauria, Sauropoda) from Texas: new perspective
613 on the relationships of North America's last giant sauropod. *Journal of Systematic*
614 *Palaeontology*. 15(5):1–26. doi:10.1080/14772019.2016.1183150.
- 615 Upchurch, P., Barrett, P.M. & Dodson, P. 2004. Sauropoda. In: Weishampel, D.B.,
616 Dodson, P., & Osmolska, H. (Eds.) *The Dinosauria* (2nd Edition). Berkeley:
617 University of California Press. Pp. 259–322.
- 618 Veroslavsky, G.; Aubet, N.; Martínez, S.; Heaman, L.M.; Cabrera, F. & Mesa, V. 2019.
619 Late Cretaceous stratigraphy of the southeastern Chaco-Paraná basin (“Norte Basin”
620 - Uruguay). The Maastrichtian age of the calcretization process. *Geociências*, 2019 ;
621 38(2):427-449
- 622 Wilson, J.A. & Sereno, P.C. 1998. Early evolution and higher-level phylogeny of
623 sauropod dinosaurs. *Society of Vertebrate Paleontology Memoirs* 5:1–68.
- 624 Zaher, H., Pol, D., Carvalho, A.B., Nascimento, P.M., Riccomini, C., Larson, P., et al.
625 2011. A Complete Skull of an Early Cretaceous Sauropod and the Evolution of
626 Advanced Titanosaurians. *PLoS ONE* 6(2): e16663. [https://doi.org/10.1371/](https://doi.org/10.1371/journal.pone.0016663)
627 [journal.pone.0016663](https://doi.org/10.1371/journal.pone.0016663)

628 Zurriaguz, V. & Cerda, J.I. 2017. Caudal pneumaticity in derived titanosaurs (Dinosauria:
629 Sauropoda). *Cretaceous Research* 75:101-114.

630 Wilson, J.A. & Upchurch, P. 2009. Redescription and reassessment of the phylogenetic
631 affinities of *Euhelopus zdanskyi* (Dinosauria:Sauropoda) from the Early Cretaceous
632 of China. *Journal of Systematic Palaeontology*. 7(2):199–239.

633

634

635

Journal Pre-proof

636 **FIGURE CAPTIONS**

637

638 Figure 1. Relations of the Cretaceous stratigraphic units from Norte Basin, Uruguay.

639 Modified from Veroslavsky et al. (2019).

640

641 Figure 2. Simplified geology of the area based in Bossi & Ferrando (2001). Black star
642 shows the location of the type-locality of *Udelartitan celeste*. Coordinates: 31° 58' 34''S,
643 55°57'43''W. Geological map taken from Bossi & Ferrando (2001). Inset shows
644 Paysandú department in Uruguay.

645

646 Figure 3. A, general view of the gully. B, silicified conglomerates. C, sandstones.

647

648 Figure 4. Titanosaur skeleton with coloured recovered elements of *Udelartitan celeste*
649 gen. et sp. nov. Holotype indicated in green. Typical Uruguayan Carnival drummer and
650 dancer for scale.

651

652 Figure 5. FC-DPV 3595 (holotype of *Udelartitan celeste* gen. et sp. nov.). First caudal
653 centrum in left lateral (A), dorsal (B) and posterior (C) views. Scale bar equals 5 cm.
654 Abbreviations: cd, condyle. ct, cotyle. lf, lateral foramina. tp, transverse process.

655

656 Figure 6. FC-DPV 3595 (holotype of *Udelartitan celeste* gen. et sp. nov.) . Second and
657 third anterior caudal centra in right lateral (A, F), ventral (B, G), dorsal (C, H), anterior

658 (D, I) and ventral (E, J) views. Scale bar equals 5 cm. Abbreviations: cd, condyle. tp,
659 transverse process. vf, ventral foramina.

660

661 Figure 7. *Udelartitan celeste* gen. et sp. nov. referred material. FC-DPV 1900. Middle
662 caudal centra in left lateral (A, F), ventral (B, G), dorsal (C, H), anterior (D, I) and ventral
663 (E, J) views. Scale bar equals 5 cm. Abbreviations: cd, condyle. dt, dorsal tuberosity. na,
664 neural arch.

665

666 Figure 8. *Udelartitan celeste* gen. et sp. nov. referred material. FC-DPV 1900. Posterior
667 caudal centra in right lateral (A, E), anterior (B, F), ventral (C, G) and posterior (D, H)
668 views. Scale bar equals 5 cm. Abbreviations: cd, condyle. na, neural arch.

669

670 Figure 9. *Udelartitan celeste* gen. et sp. nov. referred material. FC-DPV 1900. Anterior
671 caudal neural spine in right lateral (A), posterior (B), anterior (C) and dorsal (D) views.
672 Scale bar equals 5 cm. Abbreviations: posl, postpinal lamina. posz, postzygapophysis.
673 prsl, prespinal lamina. spol, spinopostzygapophyseal lamina,

674

675 Figure 10. *Udelartitan celeste* gen. et sp. nov. referred material. FC-DPV 1900 Juvenile
676 anterior caudal centra in right lateral (A), anterior (B), ventral (C), dorsal (D) and
677 posterior (E) views. Scale bar equals 5 cm.

678

679 Figure 11. *Udelartitan celeste* gen. et sp. nov. referred material. FC-DPV 1900. A, left
680 coracoid in medial view. B-C, proximal tibia in lateral (B) and proximal (C) views. D-E,
681 distal tibia in distal (D) and posterior (E) views. F-G, proximal fibula in anterior (F) and
682 proximal (G) views. Scale bars equal . Abbreviations: asap, articular surface for the
683 ascending process. cc, cnemial crest. cf, coracoidal foramen. cmr, cranomedial ridge. gl,
684 glenoid. lm, lateral malleolus. mm, medial maleollus. tp, tibial prominence.

685

686 Figure 12. *Udelartitan celeste* gen. et sp. nov. referred material. FC-DPV 1900. Large
687 and small astragali in distal (A, B), posterior (C, D), proximal (E, F), anterior (G, H) and
688 lateral (I, J). Scale bar equals 5 cm. Abbreviations: ap, ascending process. faf, facet for
689 articulation of fibula.

690

691 Figure 13. *Udelartitan celeste* gen. et sp. nov. referred material. FC-DPV 1900. Right
692 metatarsal II in anterior (A), posterior (B), proximal (C) and distal (D) views. Left
693 metatarsal II in anterior (E), posterior (F), proximal (G) and distal (H) views. Left
694 metatarsal I in anterior (I), posterior (J), proximal (K) and distal (L) views. Left metatarsal
695 IV in anterior (M), posterior (N), proximal (O) and distal (P) views. Right metatarsal I in
696 anterior (Q), posterior (R), proximal (S) and distal (T) views. Left metatarsal V in anterior
697 (U), posterior (V), proximal (W) and distal (X) views. Scale = 5 cm. Abbreviations: r,
698 ridge.

699

700 Figure 14. Excerpts of phylogenetic trees (see complete topologies in the Supplementary
701 Material) depicting the position of *Udelartitan celeste* gen. et sp. nov. A-B, Reduced strict
702 consensus trees based on the data-matrix modified from Cerda et al. (2022), analysed

703 under EWA (A) and IWA (B). C-D, Consensus trees based on the data-matrix modified
704 from Navarro et al. (2022); C, reduced strict consensus of MPTs analysed under EWA.
705 D, strict consensus of MPTs analysed under IWA. Yellow and green highlight
706 respectively indicate Saltasuroidea (or “Saltasuroidea branch”) and Saltasauridae.

707

708 Figure 15. Map of southern South America showing distribution of saltasauroids with
709 first biconvex caudal vertebra (7th sacral in the case of *Neuquensaurus*). Upper Cretaceous
710 deposits discussed in text (Paysandú, Neuquén and Baurú Groups) are depicted in red.

711 ~~Figure 15. Hypothetical restoration of *Udelartitan celeste*.~~

712

713

Table 1. Measurements (in mm) of *Udelartitan celeste*.

Condylar convexity measurements (selected vertebrae; for other measurements see Soto et al. 2012)

Anterior vertebrae [Fig. 5 y 6]

0.54, 0.76, 0.99

Middle vertebrae [Fig. 7]

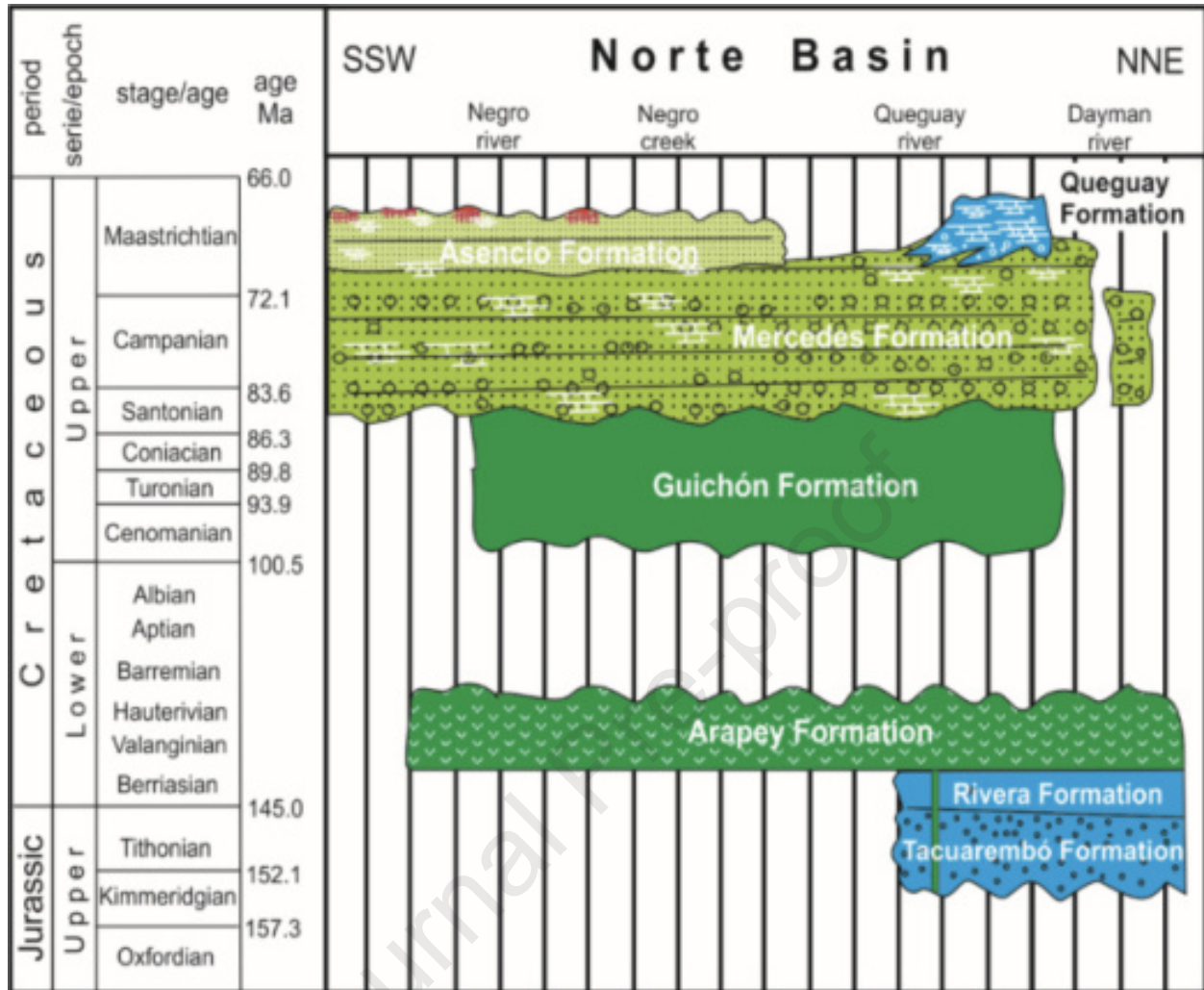
0.47, 0.5

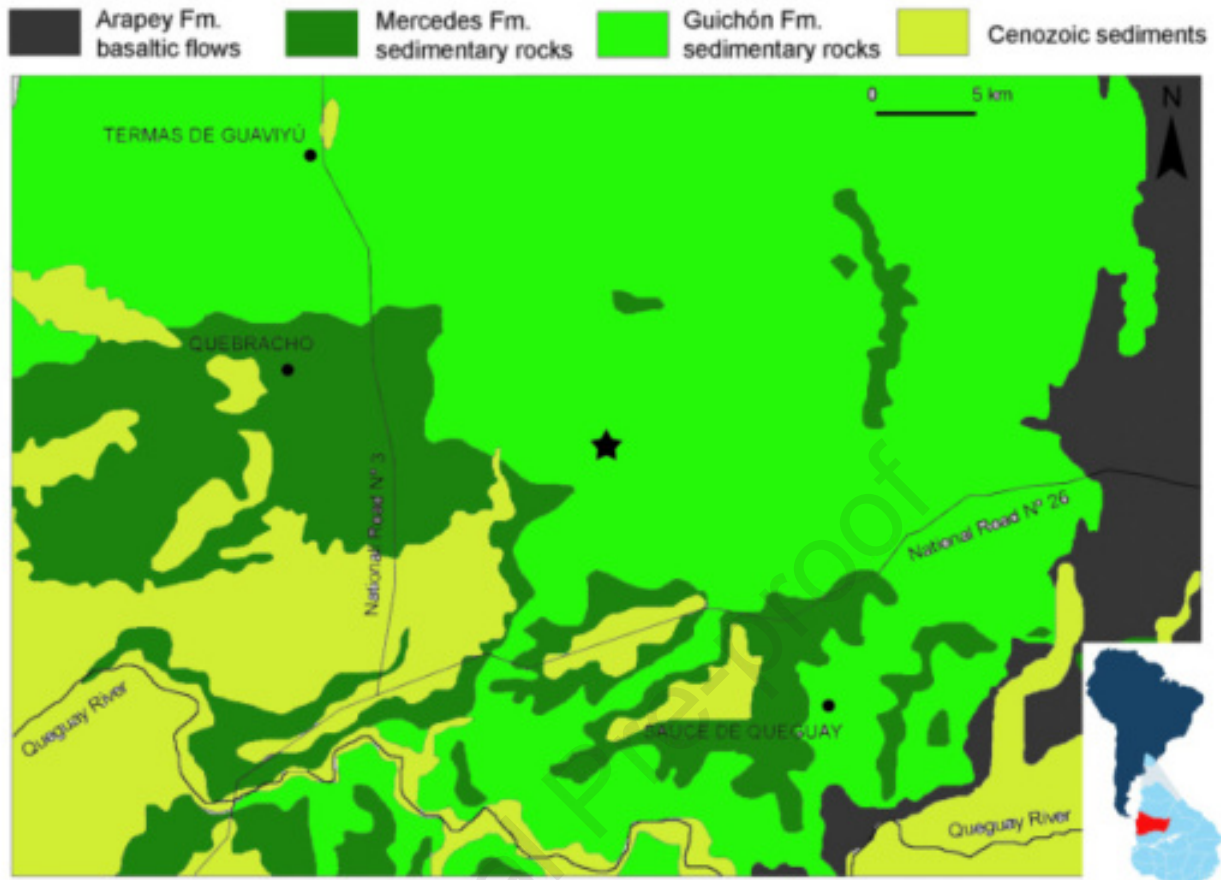
Posterior vertebrae [Fig. 8]

0.86, 0.69

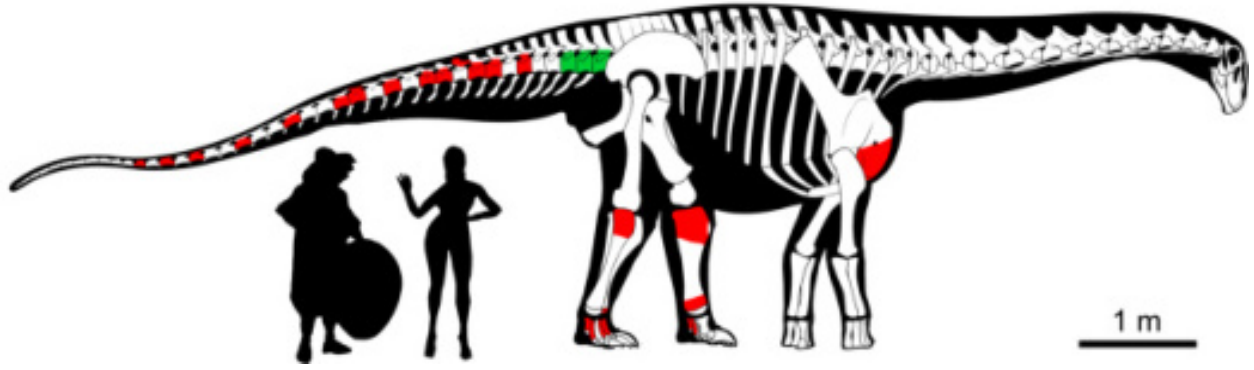
	Maximum preserved length	Anteroposterior	Mediolateral	
Proximal fibula	147.64	87.07	116.33	
Distal tibia	136.00	110.72	155.00	
	Anteroposterior (length)	Mediolateral (width)	Proximodistal (height)	
Small astragalus	82.53	128.74	71.69	
Large astragalus	107.51	150.41	88.71	
	Length	Minimum width (mid-shaft)	Maximum width (proximal)	Maximum width (distal)
Right metatarsal I	129.87	66.41	117.59	79.05
Left metatarsal II	117.83	76.30	113.50	82.51
Left metatarsal I	133.47	70.28	84.54	110.43
Right metatarsal II	118.46	63.12	70.80	80.17
Left metatarsal IV	96.89	64.14	89.73	78.15
Left metatarsal V	95.42	55.23	85.43	57.22

Journal Pre-proof

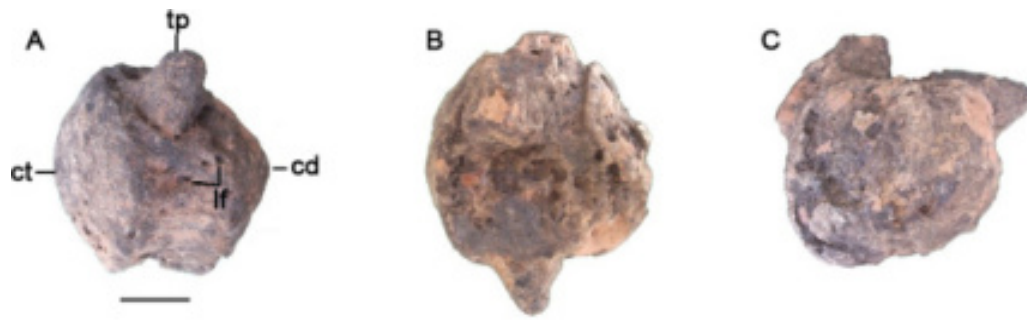




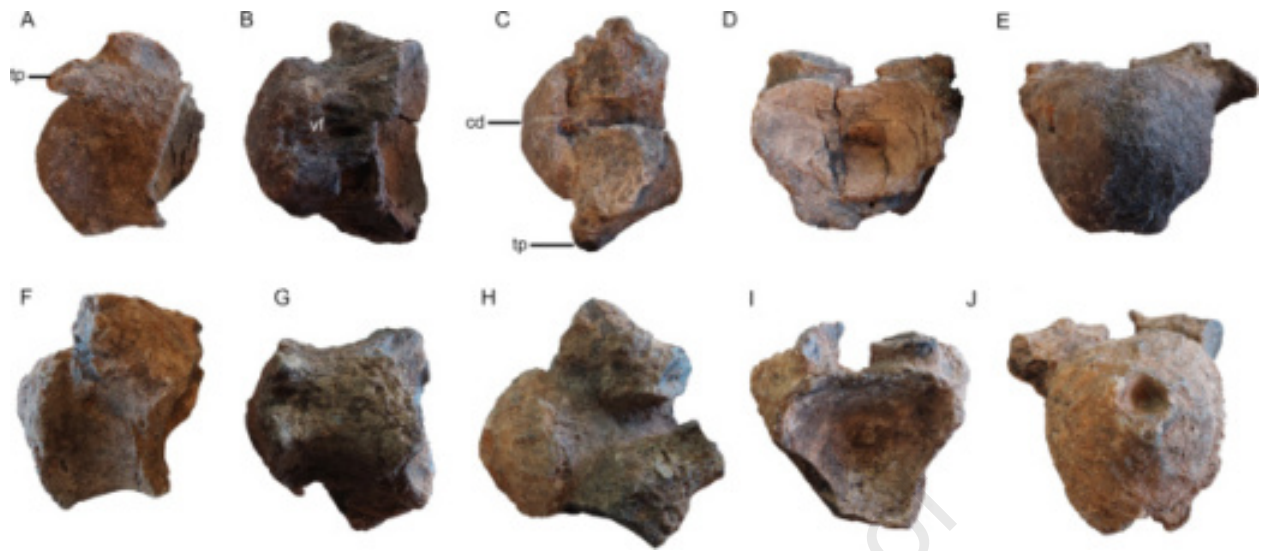




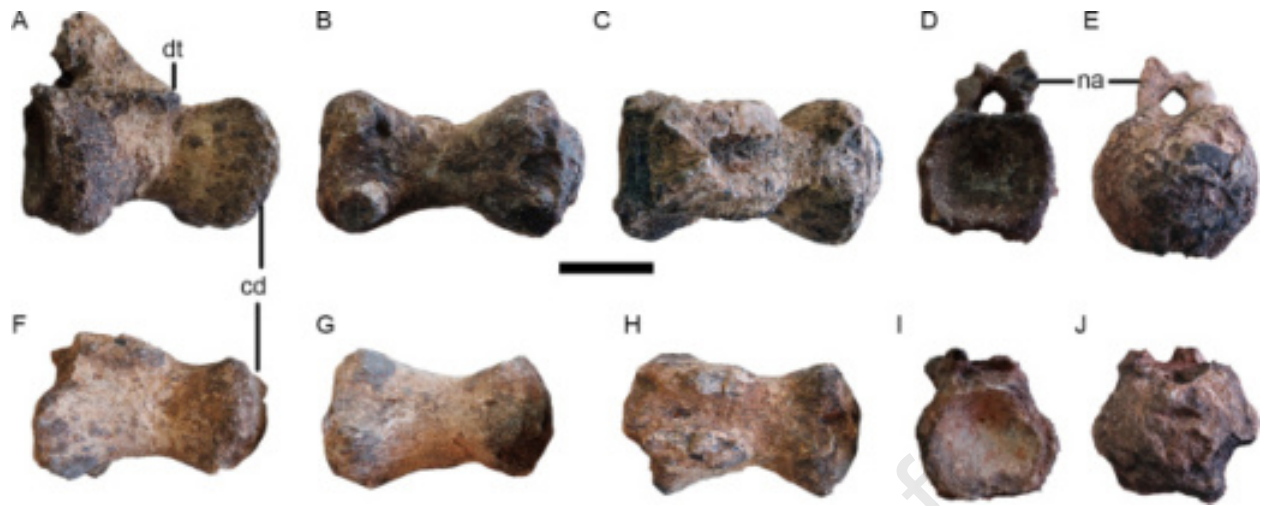
Journal Pre-proof

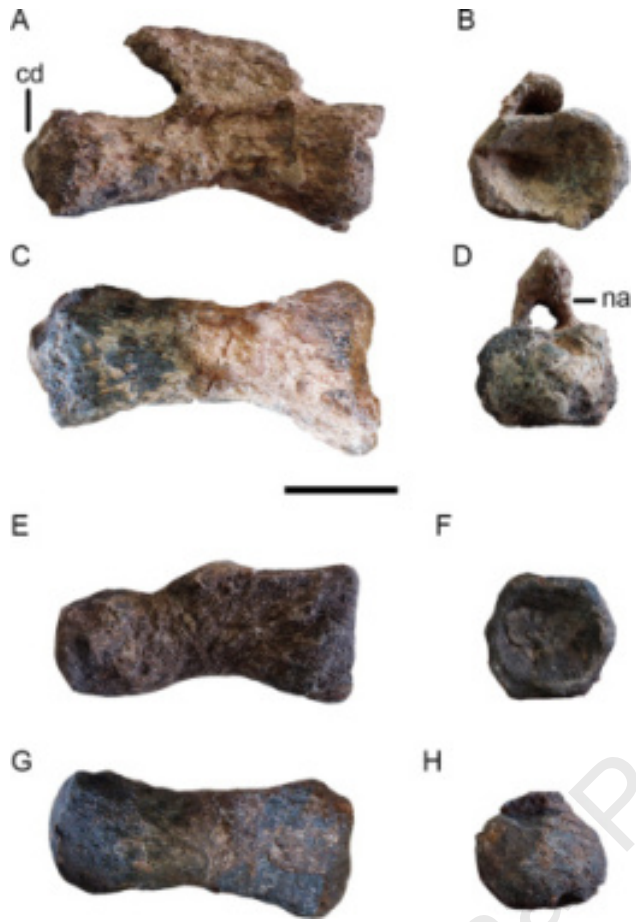


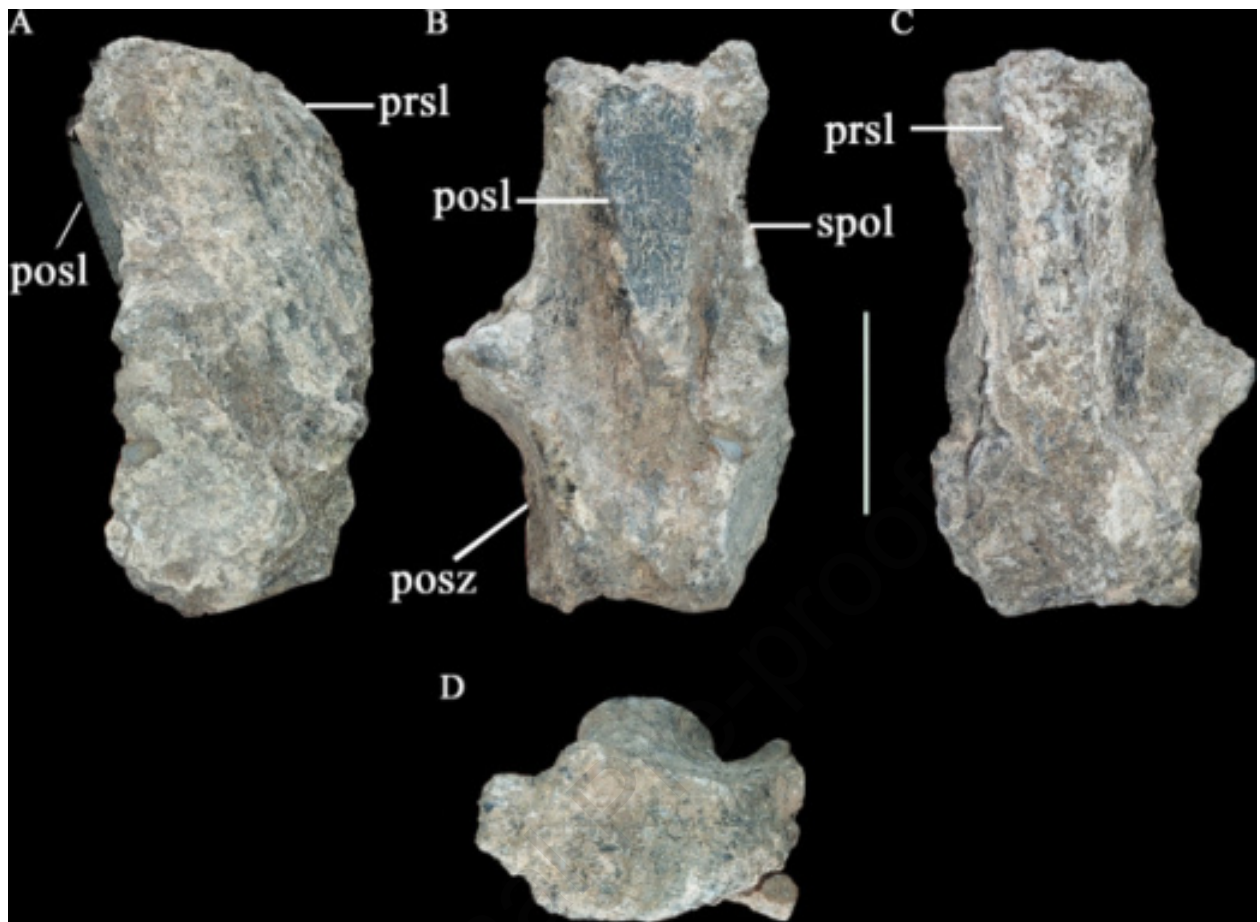
Journal Pre-proof



Journal Pre-proof







A



B



C



D



E



